Materials Transactions, Vol. 43, No. 8 (2002) pp. 1979 to 1984
Special Issue on Bulk Amorphous, Nano-Crystalline and Nano-Quasicrystalline Alloys IV

High Strength Magnesium-based Glass Matrix Composites

Birgit Bartusch, Frank Schurack and Jürgen Eckert

IFW Dresden, Institute for Metallic Materials, P.O. Box 27 00 16, D-01171 Dresden, Germany

Magnesium-based glass matrix composites containing oxide particles were produced by mechanical alloying of $Mg_{55}Cu_{30}Y_{15}$ elemental powder mixtures with the addition of MgO, CeO_2, Cr_2O_3 or Y_2O_3 oxide particles. The formation of the glassy phase was characterized by X-ray-diffraction and transmission electron microscopy methods and was found to proceed almost unaffected by the presence of the oxides. Differential-scanning-calorimetry-analysis revealed, that the amorphous matrix features a wide supercooled liquid region with an extension of about 40–50 K. Differences in the thermal stability of the composites depending on the oxide addition are discussed. Viscosity measurements proved the existence of a characteristic minimum of viscosity in this temperature range which was used to consolidate the powders into bulk samples by uniaxial hot pressing. The deformation behaviour under compression at room temperature as well as at elevated temperature of 423 K yielded excellent properties compared to conventionally produced magnesium-based alloys.

(Received February 22, 2002; Accepted May 2, 2002)

Keywords: *magnesium alloys, metallic glasses, composites, mechanical alloying, mechanical properties*

1. Introduction

The need for high strength and damage tolerant low density materials for the aerospace and automotive industry has raised comprehensive research activities devoted to the processing of light-weight aluminium and magnesium based alloys during the past thirty years.[1)] More or less as a fringe subject of the research on solid solution and precipitation hardened Al-alloys, investigations on non-equilibrium aperiodic phases such as amorphous phases have been initiated in the 70's.[2)] Today, one of the most intensely explored features of amorphous phases are their mechanical properties. Metallic glasses exhibit high hardness, very high resistance against abrasive wear and high strength, *e.g.* 2–3 times higher for Mg-based glasses compared to commercial Mg-alloys.[3)] However, at room temperature they break in a brittle fashion with almost no plastic deformation, whereas at elevated temperatures around the glass transition they show ductility of up to 20%.[4,5)] A further interesting feature of metallic glasses is the rather low elastic modulus in combination with the high proof strength compared to steels, which allows high elastic amplitudes under high loads.[6)]

Recent developments of glass-forming Mg-alloys with very good glass-forming ability and high thermal stability of the supercooled liquid against crystallization allowed the preparation of Mg-based bulk glasses.[7)] Such alloys were produced in dimensions of millimeter-sized rods or sheets by slow cooling from the melt using a copper mould casting technique.[7–9)] The mechanical properties of these metallic glasses can be furthermore improved by nanoscale precipitates or by homogeneously distributed insoluble fibers or particles.[10–12)] The idea behind this is to hinder shear band propagation and, thus, to impede the begin of deformation.[13)] Furthermore, due to the initiation of multiple shearing events a more homogeneous deformation mode can be expected. The strengthening effectivity of the particles which are either initially added elemental particles, crystallization-induced intermetallic crystallites or oxide particles depends only little on their nature but more on their size and distribution.[10,14)] Nevertheless, oxide particles were found most suitable,[15,16)] since their high intrinsic stability and, hence, a low dissolution tendency they do least affect the formation process and the thermal stability of the glassy matrix.[12)] However, upon slow cooling from the melt those additives can act as prefered sites for heterogeneous nucleation, thus, deteriorating the castability and hence, the thermal stability of the glass. Alternatively, mechanical alloying allows to prepare glass composites due to the completely different reaction temperatures and timescales for phase formation through solid state reaction.[17)] The existence of the characteristic viscosity minimum in the temperature range of the supercooled liquid offers furthermore a narrow but effective processing window for the consolidation of the powders into bulk specimens.

In the present paper, we report on the formation and the properties of mechanically alloyed MgCuY-based metallic glass composites with oxide particle additions, showing that the thermal stability of the supercooled liquid can be maintained in the presence of nanosized particles. The effectivenes of the particle addition on the improvement of the mechanical properties has been investigated.

2. Experimental Procedure

The mechanical alloying started from elemental Mg, Cu and Y powders with nominal purities of 99.9 at% for Cu, Mg and Y (nominal particles sizes $<150\,\mu m$). All powder handling was done in a glove box under argon atmosphere (O_2, H_2O $<$ 1 ppm). For the composite samples the elements were mixed to give a composition of $Mg_{55}Cu_{30}Y_{15}$ and blended with different volume percents of MgO, CeO_2, Cr_2O_3 or Y_2O_3 oxide particles with a nominal purity of 99.5 at% (nominal particles sizes $<2.5\,\mu m$). The powders were milled in a RETSCH planetary ball mill at rotational velocities of 180 rpm for different times using hardened steel milling tools and a ball-to-powder weight ratio of 13:1. Ion-coupled plasma (ICP) and atomic-absorbtion spectroscopy (AAS) analysis of the as-milled powders revealed iron impurity of less than 0.5 at% due to wear debris from the milling tools. The oxygen content of dispersoid-free powders, which mainly stem from the starting materials, was determined by

hot extraction (C436 LECO analyser) to be $\leq$0.3 mass%. The compaction of the glassy powders was done by uniaxial pressing under a vacuum of $2 \cdot 10^{-4}$ mbar at pressures up to 500 MPa at a temperature of 40 K below the onset of crystallization (T_x).

The microstructure was characterized by X-ray diffraction (XRD) using a Philips PW1050 diffractometer with Co–Kα radiation ($\lambda = 0.178896$ nm) and transmission electron microscopy (TEM) using a Philips CM20 FEG analytical microscope with 200 kV acceleration voltage. The thermal stability of the samples was analyzed by differential scanning calorimetry (Perkin-Elmer DSC7) at a heating rate of 40 K/min under flowing argon. The viscosity of the powders was analyzed by parallel-plate rheometry using a Perkin-Elmer TMA7e analyser with quartz penetration probe at a static load of 2.6 N under argon atmosphere at a heating rate of 10 K/min. Before, the glassy samples were pre-annealed above the glass transition temperature (T_g) to obtain relaxed isoconfigurational states.

Mechanical properties were tested by microhardness measurements in a Vickers microhardness tester with a static load of 0.4905 N. Ten indentations were used to determine average hardness values. Square-shaped specimens with sizes of $3 \times 3 \times 5.5\,\mathrm{mm}^3$ were prepared from the bulks and deformed under a constant compression rate of $\dot{\varepsilon} = 10^{-4}\,\mathrm{s}^{-1}$ using an Instron 8562 dynamic testing system. In order to avoid effects of friction between the sample and the punches, the contact area was bridged with teflon stripes.

3. Results and Discussion

3.1 Microstructure formation

With respect to previous investigations,[18] which revealed that for MgCuY powder mixtures the amorphization during mechanical alloying proceeds in a similar way as for binary systems[19] or other multicomponent glass-forming alloys[17] via interdiffusion in a mechanically formed arrangement of thin elemental layers, the influence of an initial addition of oxide particles on the amorphization process was studied.

The XRD patterns in Fig. 1 illustrate the phase formation after 60 h of milling starting from elemental powder mixtures for a plain $Mg_{55}Cu_{30}Y_{15}$ alloy and for powder blends of a $Mg_{55}Cu_{30}Y_{15}$ mixture with 5 vol% MgO, CeO_2, Cr_2O_3 or Y_2O_3, respectively. It clearly shows the formation of an amorphous phase for all samples. For the oxide-free reference powder, the broad amorphous halo is superimposed with peaks reflecting unreacted Mg, Cu and Y which remained present even after very long milling times. Most likely, thin oxide layers covering the grain boundaries and the particle surfaces of the highly reactive powders are present, similar as in the case of mechanically attrited nanocrystalline aluminium.[19] This prevents complete alloying even after extended milling. Hence, the high reactivity of the elements prevents the formation of a homogeneous amorphous alloy and even the dispersoid-free sample has rather to be considered as a composite of amorphous matrix and nanoscale elemental particles and oxides. Similar results were found for a variety of alloys with different compositions.[20] Although these remains are also existent in the oxide-containing powders, they appear less pronounced in the XRD patterns since

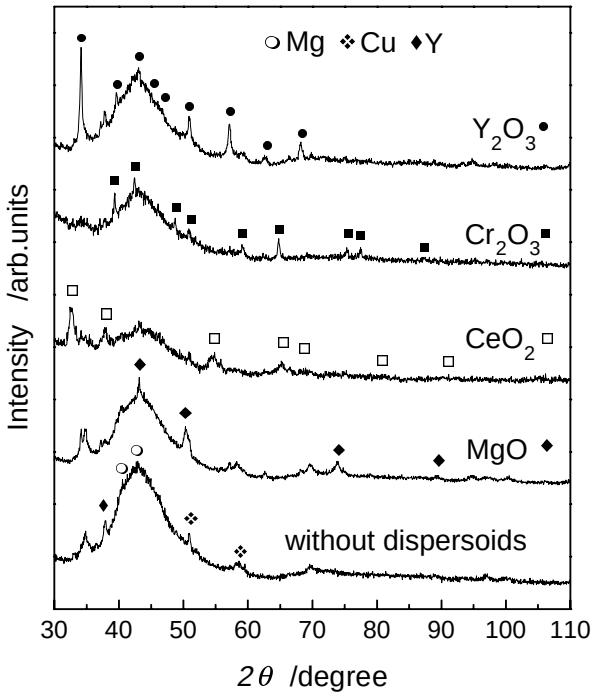

Fig. 1 XRD patterns of mechanically alloyed $Mg_{55}Cu_{30}Y_{15}$ powders without dispersoids and with addition of 5 vol% MgO, CeO_2, Cr_2O_3 or Y_2O_3 oxide powders after 60 h of milling. The oxide peaks are superimposed on the broad halo of the glassy matrix.

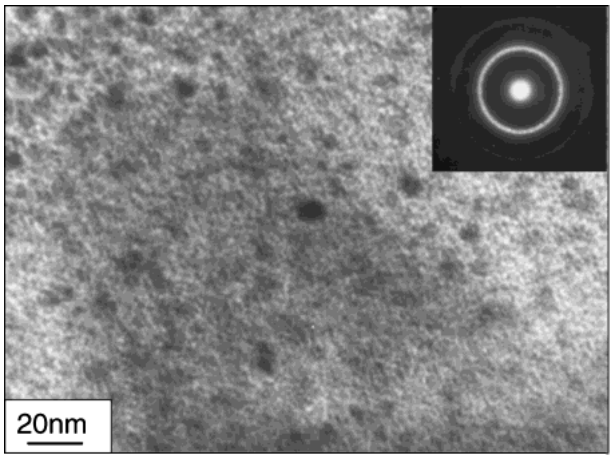

Fig. 2 Bright-field TEM image of an $Mg_{55}Cu_{30}Y_{15}$ powder sample with a dispersion of 5 vol% Y_2O_3 with an approximate particle size of 5–10 nm. The electron-diffraction pattern shows diffuse halos stemming from the amorphous matrix and an angular distribution of crystalline reflexes coming from the oxides.

the reflections are covered by the dominant oxide peaks. Intermetallic phases were not detected in any of the samples. TEM investigations confirmed the formation of an amorphous phase coextisting with nanoscale crystals with an average grain size of about 10 nm. This is shown exemplarly in Fig. 2 for $Mg_{55}Cu_{30}Y_{15}$ powder containing 5 vol% Y_2O_3 as a fine dispersion of particles in the amorphous matrix.

In the XRD patterns no displacements of the maximum of the amorphous halo were observed within the range of the experimental accuracy, as it was previously reported for $Mg_{55}Cu_{30}Y_{15}$ powders milled with initial elemental additions.[16,20] This suggests that there is no significant dissolution of the oxide particles and, hence, no shift of the matrix

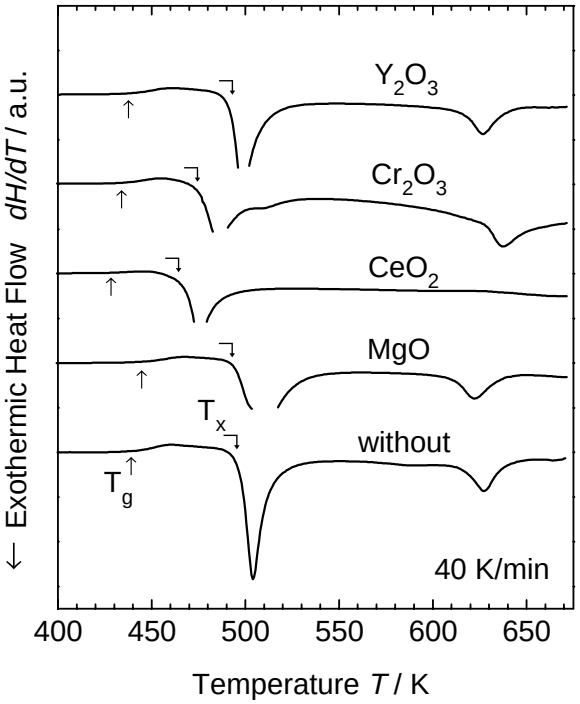

Fig. 3 DSC traces of mechanically alloyed $Mg_{55}Cu_{30}Y_{15}$ powders without dispersoids and with the addition of 5 vol% MgO, CeO_2, Cr_2O_3 or Y_2O_3 oxide powders after 60 h of milling. The characteristic temperatures of the glass transition, the onset of crystallization and the corresponding transformation enthalpies are given in Table 1.

stoichiometry.

However, the investigation of the thermal stability of the powders by DSC analysis reveals that the addition of oxides can indeed have an effect on the stability of the glassy matrix. Figure 3 compares characteristic DSC scans for as-milled powders with and without oxide addition. All samples exhibit a glass transition before crystallization, revealing that the addition of oxides does not suppress the transition from the amorphous solid to the supercooled liquid state. Thus, the amorphous matrix in these composites can be described as a glassy phase. The samples crystallize in two steps, where the primary crystallization leads to the precipitation of Mg_2Cu nanocrystals. This results in a change of the composition of the remaining matrix which crystallizes subsequently into an intermetallic phase mixture.[21] The glass transition temperatures T_g, the crystallization temperatures T_x, the extension of the supercooled liquid region $\Delta T_x = T_x - T_g$ and the enthalpy values for the primary crystallization ΔH_x are given in Table 1 (T_g and T_x are defined as the onset temperatures of the respective reaction in the DSC scan). The results for the dispersoid-free powder are consistent with data for rapidly quenched MgCuY ribbons or cast alloys.[8,9,22]

Although the main features are equal for all the powders, there are differencies in T_g, T_x, ΔT_x and ΔH_x between the plain powder and the composite powders. For the composite containing 5 vol% Y_2O_3, the glass transition of 439 K and the onset of crystallization of 494 K are almost identical with values for the dispersoid-free powder ($T_g = 441$ K, $T_x = 497$ K) within the accuracy of the measurement. Also the enthalpies of crystallization are with 2.33 kJmol^{-1} and 2.29 kJmol^{-1} about the same for both samples, respectively. Similar results were found for the MgO containing composite. This indicates, that these oxides remain stable and do not degrade the thermal stability of the matrix. In contrast, blends with 5 vol% of CeO_2 or Cr_2O_3 however show a slightly lower T_g and, more important, a reduced T_x, resulting in a decrease of ΔT_x to about 40 K. This suggests that the CeO_2 and Cr_2O_3 particles dissolve upon milling, thus changing the overall stoichiometry of the glassy matrix and, consequently, its thermal stability. The change in the onset temperature and the reaction enthalpy of the secondary crystallization for the Cr_2O_3 composite and its complete suppression for the CeO_2-containing powder corroborate this conclusion. Since also in these powders Mg_2Cu precipitates during the primary reaction, the composition of the remaining matrix has been changed for all the samples in about the same way. Therefore, the appearent differencies of the final crystallization of the remaining matrix in the second step gives evidence for a change in the matrix stoichiometry due to the dissolution of CeO_2 and Cr_2O_3 particles. Nevertheless, all samples maintain a rather wide supercooled liquid region.

Similar investigations[16] on the influence of the particle volume fraction on the formation of an amorphous phase showed for Y_2O_3 additions, that the appearance of an extended supercooled liquid region in the presence of oxide particles is not restricted to small oxide volume fractions only. Even at high concentrations of up 30 vol% the formation of the amorphous phase proceeds unaffected. Moreover, the glass transition temperature as well as the onset of crystallization and the enthalpy do not change significantly. Comparing the dispersoid-free sample and the composite samples, isothermal DSC measurements (not shown here) revealed furthermore similar incubation times for the onset of crystallization but significantly shorter times for the reaction itself.[21,23] This supports the conclusion that although the enhanced number of potential nucleation sites affects the transformation kinetics once the reaction started, it does not promote the begin of the crystallization reaction by interface-controlled nucleation at the Y_2O_3-matrix phase boundary. Obviously, the Y_2O_3 particles do neither deteriorate the conditions for an effective alloying process nor do they act effectively as heterogeneous nucleation sites, triggering massive crystallization.

3.2 Viscosity measurements, powder consolidation

The characteristic softening of a glassy phase in the temperature range of the supercooled liquid can be exploited for the consolidation of metallic glass powders. Figure 4 shows viscosity measurements for dispersoid-free $Mg_{55}Cu_{30}Y_{15}$ and for the different composites as obtained from parallel plate rheometry measurements. The viscosity η in these measurements is not an intrinsic property of the glassy phase but must be considered as an average value including the contribution of the oxides and the fractions of unreacted material. The scans show the typical decrease in viscosity with temperature upon heating through the glass transition. At elevated temperatures the viscosity increases significantly due to the start of crystallization. The measured viscosities are consistent with the data for cast MgCuY bulk glasses[22] and for Zr-based glass matrix composites.[11,24,25] Compared to the results of the DSC scans, there are similar differences in the thermal behaviour between the different powders mainly concerning

Table 1 Summary of characteristic thermophysical data measured by DSC on powders and mechanical data obtained from constant rate compression tests of bulk specimens of amorphous $Mg_{55}Cu_{30}Y_{15}$ samples with 5 vol% particle addition of different oxides at room temperature. (T_g-glass transition temperature, T_x-crystallization temperature, ΔT_x-temperature range of the supercooled liquid, ΔH_x-crystallization enthalpy, H_V-Vicker's hardness, σ_f-fracture strength, ε_f-fracture strain, E-Young's modulus).

Dispersoids	T_g/K	T_x/K	ΔT_x/K	ΔH_x/kJmol^{-1}	H_V/GPa	σ_f/GPa	ε_f/%	E/GPa
Without	441	497	56	−2.33	3.45	553	1.8	32
MgO	443	494	51	−2.38	3.75	390	1.4	40
CeO_2	428	468	40	−1.51	3.88	595	1.9	36
Cr_2O_3	434	475	41	−1.92	3.68	609	1.1	70
Y_2O_3	439	494	55	−2.29	3.85	709	1.6	60

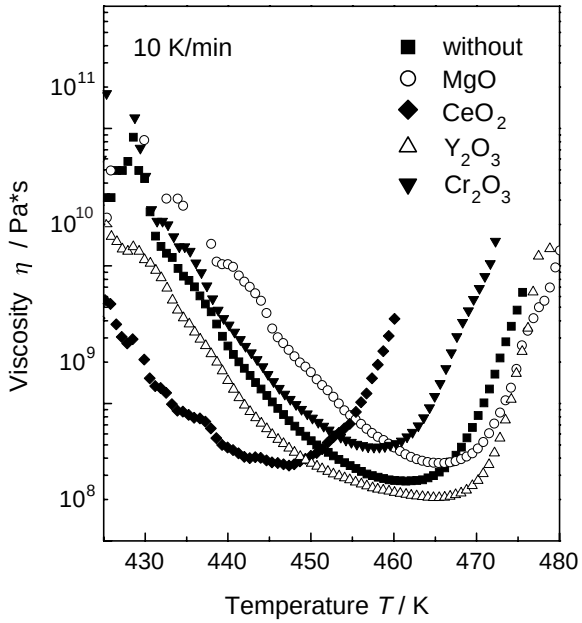

Fig. 4 Viscosity of mechanically alloyed $Mg_{55}Cu_{30}Y_{15}$ powders without dispersoids and with the addition of 5 vol% MgO, CeO_2, Cr_2O_3 or Y_2O_3 oxide powders after 60 h of milling. (heating rate 10 K/min).

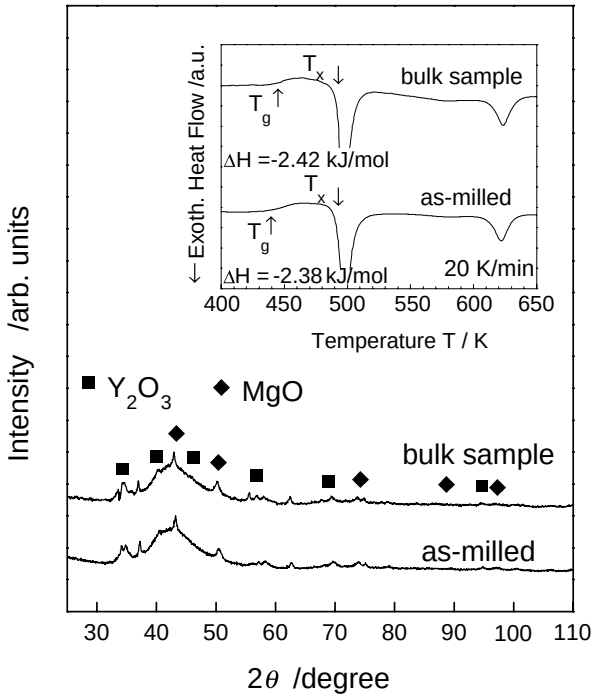

Fig. 5 Comparison of the XRD patterns of as-milled $Mg_{55}Cu_{30}Y_{15}$ powder with 5 vol% MgO and of the same powder after compaction by uniaxial hot pressing at 454 K. The inset shows the corresponding DSC scans.

the temperatures of glass transition and crystallization, which are related to the compositional changes of the matrix due to oxide dissolution. Although the presence of nanoscale oxide particles generally leads to a retardation of viscous flow in the supercooled liquid region,[11,24] the difference in the viscosity minimum and the temperature characteristics is rather small as it can be concluded from Fig. 4. Previous studies of the thermal stability of $Mg_{55}Cu_{30}Y_{15}$ samples with up to 30 vol% of Y_2O_3[16] showed, that significant changes of the overall flow behaviour, *e.g.* the minimum viscosity in the supercooled liquid region, only occur for particle volume fractions of 10 vol% and higher. More important, the distinct viscosity decrease offers a quite comfortable processing window for the consolidation of the powders by hot pressing. Moreover, as-compacted bulk samples can be further deformed or shaped in the respective temperature range.

Based on these results, the powders were consolidated into bulk samples of up to 20 mm in diameter and 6 mm in height by uniaxial hot pressing. In order to make use of the decrease in viscosity, but also to avoid isothermal crystallization, the compaction was performed at a temperature of $T_x - 40$ K. The comparison of the microstructure of as-milled powder and hot pressed bulk samples by XRD analysis (see Fig. 5) did not give any hint for crystallization upon powder consolidation. The finding of almost equal crystallization enthalpies as a measure for the reacted volume fraction and similar temperature features in the DSC analysis, as it can be seen in the inset in Fig. 5 for $Mg_{55}Cu_{30}Y_{15}$–MgO composites, give further evidence that the phase composition remained unchanged upon compaction. The density of the compacted bulks was determined by Archimedes method to be more than 99.5%.

3.3 Mechanical properties

The mechanical properties were investigated by Vickers microhardness (H_V) tests and constant rate compression tests. The H_V values vary between 3.45 GPa and 3.88 GPa for the oxide-free material and the oxide-containing powder, respectively (see also Table 1). No cracks were observed radiating from the edges or sides of the indentations, indicating a rather high fracture toughness of the material. Compared with the values of 2.0 to 3.2 GPa for rapidly quenched MgCuY amorphous alloys the hardness of the present consolidated powders is larger and about in the range of the hardness of partially or fully crystallized ribbons (3.9 to 4.3 GPa) of the same or com-

parable composition.[9] This must be explained as a strengthening effect of the nanometer-sized oxide particles and unreacted constituents in the mechanically alloyed samples.

In Table 1, data of the Young's modulus E, the fracture strength σ_f and the fracture strain ε_f for a plain $Mg_{55}Cu_{30}Y_{15}$ glassy bulk sample and different bulk composites at room temperature are summarized. As a characteristic feature, all samples show very high strength values with a maximum of 709 MPa for the Y_2O_3 composite. However, they fracture in a brittle fashion without evidence for plasticity at room temperature. Furthermore, the elastic modulus E increases as a result of oxide particle addition. Due to this high material brittleness the specimens are very sensitive against any preparation artefacts like larger oxide inclusions or pores. This is why the correlation of the overall strength values with the composite composition is not straight forward. Obviously, the degradation of the microstructure for the CeO_2- and Cr_2O_3-containing samples resulting from the discussed dissolution of oxide particles in the matrix has no pronounced influence on the mechanical properties. A possible strength contribution due to the change of the composition of the glassy matrix can therefore be neglected, at least at room temperature. Nevertheless, the room temperature strengths obtained for these samples are 1.5 to 2.5 times higher than the strength performance of state-of-the-art Mg-based cast alloys.[3]

The influence of the dispersoid volume fraction on the mechanical properties has been studied for $Mg_{55}Cu_{30}Y_{15}$ bulk composite samples with 0, 5 and 20 vol% of Y_2O_3 addition. Figure 6 shows plots of the true stress σ vs. the true compression ε for these samples resulting from compression tests at a constant compression rate of 5×10^{-4} s^{-1} at room temperature as well as at 423 K. The strengthening effect owed to the oxide dispersoids is obvious from the increase in fracture strength by about 100–150 MPa compared to the dispersoid-free specimen as well as from the considerably larger Young's modulus of 60 GPa compared to 32 GPa, respectively. The fact that the specimen with 20 vol% Y_2O_3 addition fails unexpectedly at a lower stress than the sample with only 5 vol% Y_2O_3 must be attributed to consolidation artefacts in this sample.

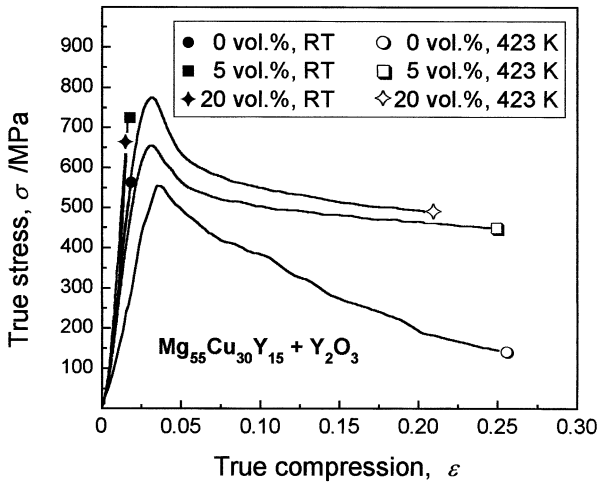

Fig. 6 Plots of the true stress vs. true compression obtained from constant rate compression tests ($\dot{\varepsilon} = 5.5^{-4}$ s^{-1}) at room temperature and at 423 K for $Mg_{55}Cu_{30}Y_{15}$ composite powders with different additions of Y_2O_3 prepared by mechanical alloying and hot pressing. The symbols indicate the point of fracture.

The strength increase due to particle addition is even more pronounced at elevated tempertures slightly below T_g. Most relevant, however, is the dramatically different deformation behaviour of the samples at 423 K, showing plasticity of up to 24%. This is owed to a change of the deformation mode in the material. At room temperature the deformation is governed by the formation and movement of localized shear bands.[26,27] Since the deformation is restricted to the volume of the shear band with a size of about 10 to several tens of nanometers, it appears to be very heterogeneous. At elevated temperatures around the glass transition the deformation is more homogeneous since each volume element contributes to deformation.[27] It can be described as a viscous flow of atoms in the entire volume and is then mainly temperature controlled. This, however, holds true only at low strain rates. At higher strain rates, *i.e.* higher than 10^{-4} s^{-1}, the stress-controlled deformation by shear band mechanism dominates, leading again to a more heterogeneous deformation. A further characteristic feature which is consistent with observations in Zr-based bulk metallic glasses[28] is the existence of a stress maximum, followed by a continuous stress reduction with increasing compression. The drop of the stress after reaching its maximum has its origin in the formation of additional free volume in the course of the deformation, leading to the softening of the material. The amount of free volume formed depends essentially on the applied load and on the deformation rate.[28]

The yield strengths at 423 K are almost equal to the room temperature strength for the oxide-free and the 5 vol% sample or even exceeds it for the 20 vol% specimen. This remarkable finding corroborates the conclusion that the room temperature strength values should be considered as the minimum achievable strength due to the high sensitivity of the brittle material against preparation artefacts at low temperature which causes failure below the true intrinsic strength of the composite material. The yield strength at 423 K does not show a simple proportional dependence on the oxide volume fraction of the composite. This corresponds to the expectation that the contribution of the oxide particles to the overall strength is rather little due to their intrinsic strength, but more since they effectively influence the deformation mechanism of the matrix. For this, the size and a homogeneous dispersion of the particles in the matrix is of much greater importance than their volume fraction. Further investigations are under way to explore the microscopic mechanism of the particle-matrix-interaction. This is, because under the assumption, that at temperatures around T_g the deformation by viscous flow of all atoms dominates, a proposed pinning of shear bands can not longer taken into consideration for a reasonable explanation of the high temperature deformation. In contrast, the suppression of shear slip in the glassy matrix due to the particle interaction as well as multiple shearing events are considered as the origin of the strength increase at room temperature, similar as for the strengthening of crystallization-induced nanoscale metallic precipitates in an amorphous matrix.[10,14]

4. Conclusions

MgCuY composites with oxide particles embedded in a glassy matrix were produced by mechanical alloying of elemental powders. Non of the additions of 5 vol% of CeO_2, Cr_2O_3, MgO and Y_2O_3 was found to affect the formation of an amorphous phase significantly. However, in all the composite powders small amounts of unreacted elemental constituents remained. Nevertheless, a $Mg_{55}Cu_{30}Y_{15}$ glassy matrix formed, revealing with a T_g of 439 K, T_x of 494 K and hence a ΔT_x of 55 K, a high thermal stability. CeO_2 and Cr_2O_3 were found to partially dissolute in the matrix and hence, to reduce the thermal stability exhibiting lower T_g and T_x as well as a smaller ΔT_x, whereas powders containing MgO and Y_2O_3 show the same features as the dispersoid-free powder. Parallel plate rheometry analysis proved the existence of a viscosity minimum in the supercooled liquid region, characteristic for metallic glasses. The softening of the material in this temperature range was used to consolidate the powders by uniaxial hot pressing at around 40 K below the crystallization point. Constant rate compression tests revealed excellent properties for the bulk specimens, yielding a maximum room temperature strength of 709 MPa in the case of the $Mg_{55}Cu_{30}Y_{15}$–5 vol% Y_2O_3 composite. This is 1.5 to 2.5 times higher than the strength performance of conventional Mg-based cast alloys. At 423 K, there was only a minor reduction in yield strength compared to room temperature, which was furthermore found to depend essentially on the oxide volume fraction.

Acknowledgements

The authors wish to thank H. Schulze and J. Klaus for technical assistance and N. Schlorke-de Boer and M. L. Seiferth for stimulating discussions. Financial support by the German Science Foundation is gratefully acknowledged.

REFERENCES

1) W. J. G. Bunk: In: *Advanced Aerospace Materials*, ed. by H. Buhl (Springer, Berlin, Heidelberg, 1992) p. 1.
2) F. E. Luborsky (ed.): *Amorphous Metallic Alloys*, (Butterworths, Boston, 1983).
3) I. J. Polmear: *Light alloys*, (E. Arnold Ltd., London, 1981).
4) F. Spaepen and A. I. Taub: In: *Amorphous Metallic Alloys*, ed. by F. E. Luborsky (Butterworths, Boston, 1983) Chap. 13.
5) T. Matsumoto and R. Madding: Mater. Sci. Eng., **19** (1975) 1.
6) C. T. Liu, L. Heartherly, D. S. Easton and A. Inoue: Mater. Trans., JIM **29** (1998) 1811.
7) A. Inoue, K. Othera, K. Kita and T. Masumoto: Jpn. J. Appl. Phys. **27** (1988) L2248.
8) S. G. Kim, A. Inoue and T. Masumoto: Mater. Trans., JIM **31** (1990) 929–934.
9) S. G. Kim, A. Inoue and T. Masumoto: Mater. Trans., JIM **32** (1991) 875–881.
10) C. Fan and A. Inoue: Mater. Trans., JIM **38** (1997) 1040–1046.
11) H. Kato and A. Inoue: Mater. Trans., JIM **38** (1997) 793–800.
12) H. Choi-Yim and W. L. Johnson: Appl. Phys. Lett. **71** (1997) 3808–3810.
13) H. Chen, Y. He, G. J. Shiflet and S. J. Poon: Nature **367** (1994) 541.
14) A. L. Greer: Curr. Opin. in Solid State & Mater. Sci. **2** (1997) 412–416.
15) A. Kuebler, J. Eckert and L. Schultz: Nanostr. Mater. **12**, 1–4 (1999) 443–446.
16) B. Weis and J. Eckert: J. Metast. Nanostr. Mater. **343–346** (2000) 129–134.
17) J. Eckert: Mater. Sci. Eng. **A226–228** (1997) 364–373.
18) J. Eckert, N. Schlorke, C. A. R. T. Miranda and L. Schultz: *Phase Formation and Properties of Mechanically Alloyed Mg-based Multicomponent Lightweight Alloys*, ed. by C. M. Ward-Close, F. H. Froes, D. J. Chellman, S. S. Cho, (The Minerals, Metals and Materials Society, Warrendale, PA, 1997) pp. 383–394.
19) J. Eckert, J. C. Holzer, C. C. Ahn, Z. Fu and W. L. Johnson: Nanostruct. Mater. **2** (1993) 407–413.
20) N. Schlorke, B. Weis, J. Eckert and L. Schultz: Nanostr. Mater. **12** (1999) 127.
21) B. Bartusch and J. Eckert: unpublished results.
22) R. Busch, W. Liu and W. L. Johnson: J. Appl. Phys. **83** (1998) 4134–4141.
23) N. Schlorke, J. Eckert and L. Schultz: *Proc. of the conference on Magnesium Alloys and Their Applications, Wolfsburg*, Germany, 1998, (Werkstoff-Informationsgesellschaft, Frankfurt/M, 1998) p. 533.
24) J. Eckert, M. Seidel, A. Kubler, U. Klement and L. Schultz: Scr. Mater. **38** (1998) 595–602.
25) J. Eckert, A. Kubler and L. Schultz: J. Appl. Phys. **85** (1999) 7112–7119.
26) F. Spaepen: Acta Metall. **25** (1977) 407.
27) A. S. Argon: Acta Metall. **27** (1979) 47.
28) A. Reger-Leonhardt, M. Heilmaier and J. Eckert: Scr. Mater. **43–5** (2000) 459–464.